

**STRETCH INDUCTION OF CYCLOOXYGENASE-2 EXPRESSION IN HUMAN  
UROTHELIAL CELLS IS CALCIUM AND PROTEIN KINASE C ZETA-DEPENDENT**

**Travis J. Jerde, William S. Mellon, Dale E. Bjorling, Celina M. Checura, Kwadwo Owusu-Ofori,  
John J. Parrish, and Stephen Y. Nakada**

The Uro pharmacology and Endourology Research Laboratory

Departments of Pharmaceutical Sciences (TJJ, WSM), School of Veterinary Medicine (CMC,  
DEB), College of Agricultural and Life Sciences (JJP) and Surgery-Division of Urology (TJJ,  
DEB, SYN)

University of Wisconsin School of Medicine and Public Health  
Madison, WI

**Running Title:** PKC $\zeta$  in stretch-induced COX-2 expression

**Address all correspondence and reprint requests to:**

Travis J. Jerde, Ph.D.

University of Wisconsin Medical School; Department of Surgery, Division of Urology

K6-561 Clinical Science Center; 600 Highland Avenue

Madison, WI 53792

Phone: 608-265-8706

Email: [jerde@surgery.wisc.edu](mailto:jerde@surgery.wisc.edu)

**Number of text pages:** 23

**Number of tables:** 0

**Number of figures:** 5

**Number of References:** 40

**Words in abstract:** 229

**Words in introduction:** 627

**Words in discussion:** 828

**Nonstandard abbreviations:** PKC, protein kinase C; COX, cyclooxygenase; NSAIDs, non-steroidal anti-inflammatory drugs; RT-PCR, reverse transcriptase-polymerase chain reaction; dNTPs, deoxyribonucleotide triphosphates; GAPDH, glyceraldehyde-3-phosphate dehydrogenase; SDS, sodium dodecyl sulfate; PAGE, polyacrylamide gel electrophoresis; FBS, fetal bovine serum;  $[Ca^{++}]_i$ , free intracellular calcium concentration; EGTA, ethylene glycol tetraacetic acid; DTT, dithiothreitol; LDH, lactate dehydrogenase; AC, adenylyl cyclase; PP, psuedosubstrate peptide; PDK, phosphoinositide-dependent kinase; PI<sub>3</sub>K, phosphoinositol-3 kinase; MAPK, mitogen-activated protein kinase

## ABSTRACT

Prostanoid synthesis via cyclooxygenase (COX)-2 induction during urothelial stretch is central to nociception, inflammation, contractility, and proliferation caused by urinary tract obstruction. We used our previously published primary human urothelial cell stretch model to evaluate the signaling mechanisms responsible for stretch-induced COX-2 expression in urothelial cells. To determine intracytosolic calcium concentrations ( $[Ca^{++}]_i$ ), primary human urothelial cells were grown on flexible membranes and loaded with Fura-2 AM. We determined  $[Ca^{++}]_i$  on a fluorescent scope during stretch. Additional cells were treated with BAPTA-AM, stretched, and COX-2 mRNA and protein were evaluated by real-time PCR and immunoblotting. To evaluate protein kinase C (PKC) in this system, cells were stretched and fractionated into membrane, cytosol, and nucleus. Fractions were immunoblotted for PKC $\alpha$ ,  $\beta$ 1, and  $\zeta$ , the predominant isoforms in urothelial cells. We treated additional cells with increasing concentrations of either bisindolylmaleimide-I or a peptide PKC pseudosubstrate inhibitor and COX-2 mRNA and protein were evaluated after stretching. Further, we transfected urothelial cells with siRNA against each of the inducible PKC isoforms in these cells and evaluated the stretch-induced COX-2 response. Stretch of urothelial cells activated calcium flux and PKC translocation to membrane and nucleus. Pharmacologic inhibition indicated that stretch-induced COX-2 expression is dependent on calcium and PKC, and biochemical knockdown experiments indicated that PKC $\zeta$  is the predominant isoform mediating stretch-induced COX-2 expression. Elucidating the signaling mechanism of stretch-induced COX-2 expression may identify therapeutic targets.

Obstructive diseases of the ureter are associated numerous deleterious effects including severe pain, inflammation, hypercontractility, cell proliferation, and potentially, cell transformation. (Gulmi et al, 1998; Weiss, 2002) Ureteral obstruction has a lifetime incidence of 13%, and total societal costs associated with diagnosis, treatment, pain management, and lost wages totals over \$2 billion annually. (Clark et al; Romello et al, 2000) There is a substantial gap in the knowledge of the physiological changes that occur during ureteral obstruction, and this has limited the development of superior pharmacologic agents for symptomatic treatment of the disease. Because of this, narcotics remain first line therapy for treatment of symptomatic ureteral obstruction despite serious side effects and addictive concerns.

Prostanoids are critical to the physiological effects associated with ureteral obstruction. (Cole et al, 1988) The rate-limiting step in prostanoid synthesis is conversion of arachidonic acid to prostaglandin (PG) G<sub>2</sub> and subsequent conversion to PGH<sub>2</sub>. (Foegh et al, 1999) This reaction is catalyzed by cyclooxygenase (COX), an enzyme that exists in two isoforms: COX-1 and COX-2. (Kujuba et al, 1991) COX-1 is present in most human tissues, and although COX-1 expression can be regulated, it is usually considered to be expressed constitutively. (Foegh et al, 1999) COX-2 is present in most tissues at low levels but is substantially induced by local inflammatory and physical stimuli in addition to its homeostatic role.

Nonsteroidal anti-inflammatory drugs (NSAIDs) inhibit prostanoid synthesis and are used effectively to treat the pain and inflammation associated with urological obstruction. (Basar et al, 1991) However, NSAIDs cause gastric ulceration, inhibit platelet aggregation, and impair renal function. (Colletti et al, 1999; Oren and Ligumsky, 1994) Selective COX-2 blockade is an

intriguing therapy for symptoms of urinary tract obstruction because these medications provide potent analgesia with fewer toxic side effects than non-selective COX inhibitors. (Lanza et al, 1999) However, selective COX-2 inhibitors are also associated with renal side effects, particularly during ureteral obstruction when renal function is compromised. (Brune and Neubert, 2001; Hernandez et al, 2002) In addition, COX-2 inhibition is associated with cardiovascular side effects and clotting in susceptible individuals. (Mukherjee et al, 2001) Elucidation of cellular mechanisms that couple distention of the urinary tract with increased COX-2 activity may identify targets of drug action directed specifically at COX-2 induction.

In vivo obstruction and distension induces COX-2 expression in the urinary bladder, ureter, and kidney. (Park et al, 1998; Nakada et al, 2002; Chou et al, 2003) Further, mechanical stretch induces COX-2 expression in numerous cell culture models including vascular endothelial cells, osteoblasts and renal podocytes. (Fitzgerald et al, 2004; Inoue et al, 2002; Martineau et al, 2004) In addition, we have recently reported a cell culture model of urothelial cell stretch-induced COX-2 expression, and found that stretch-induced COX-2 expression is regulated at both transcriptional and post-transcriptional levels. (Jerde et al, 2006)

We seek to determine the cellular mechanosensitive pathways in urothelial cells responding to during stretch that result in COX-2 induction. Deciphering the signaling mechanisms will assist in the identification of novel drug targets for the treatment of symptomatic urological obstructions. Stretch-activated calcium flux is believed to be a trigger in cellular stretch signaling. (Hamill et al, 2001) A primary effect of calcium signaling is activation of protein kinase C (PKC) signaling and recent reports have implicated PKC as critical in

mechanotransduction. (Malhaltra et al, 2001) The 11 known isoforms of PKC are divided into 4 major groups: classical ( $\alpha$ ,  $\beta 1$ ,  $\beta 2$ ,  $\gamma$ ); novel ( $\delta$ ,  $\epsilon$ ,  $\eta$ ,  $\theta$ ); atypical ( $\zeta$ ,  $\iota/\lambda$ ); and mu ( $\mu$ ). (Newton, 1995) Upon activation by calcium, classical PKC isoforms migrate to the plasma membrane or nucleus and are active as kinases. (Newton, 1995) The purpose of this study is to determine if cell stretch induces calcium flux and PKC activation (translocation), and to determine if these signaling intermediates are involved in stretch-induced COX-2 expression.

## ***MATERIALS AND METHODS***

### ***Pharmacologic agents and chemicals***

Ham's F12 nutrient medium, streptomycin/penicillin, fetal bovine serum, L-glutamine, glucose, transferrin, nonessential amino acids, and Trypsin-EDTA were purchased from Sigma-Aldrich (St. Louis, MO). Fura-2 AM, Fura-2, and the medium calcium removal kit were purchased from Molecular Probes (La Jolla, CA). BAPTA-AM, bisindolylmaleimide-1, myristoylated PKC pseudosubstrate peptide, and KT-5720 were purchased from Calbiochem (La Jolla, CA). GAPDH monoclonal antibody was purchased from Abcam (Cambridge, MA) and COX-2 monoclonal antibody was purchased from Cayman Chemical (Ann Arbor, MI). Polyclonal antibodies to all PKC isoforms were purchased from Santa Cruz Biotechnology (Santa Cruz, CA). Antibodies to Nuclear Lamin B1 and Lactate Dehydrogenase were purchased from Abcam (Cambridge, MA) and the adenylyl cyclase activity assay was purchased from Molecular Devices, Sunnyvale, CA.

### ***Isolation and culture of primary urothelial cells.***

We isolated and grew primary urothelial cells in culture as previously described. (Teng et al, 2002) Briefly, we obtained fresh human ureteral segments and placed them in supplemented Ham's F12 nutrient medium (Sigma-Aldrich, St. Louis, MO) with 5% (v/v) fetal bovine serum (FBS, Sigma), 5 µg/ml apo-transferrin (Sigma), 2.7 mg/ml glucose (Sigma), 0.1 mM nonessential amino acids (Sigma), 100 U/ml penicillin, 100 µg/ml streptomycin (Sigma), and 2

mM L-glutamine (Sigma). The ureter was opened to expose the urothelium and all fat and connective serosa was removed. The urothelial layer was manually removed, placed in fresh supplemented F12 media and minced. The tissue containing medium was transferred to a collagen-coated sterile tissue culture plate and grown in supplemented Ham's F12 for 24 hours. When cells achieved confluency, they were split by incubating with 0.25% Trypsin-EDTA (Sigma) for 10 minutes at 37°C. This high concentration of trypsin was used because the cells attached tightly to collagen. Ham's F12 with 5% FBS was added and the lifted slurry was centrifuged at 500xG for 5 minutes to collect the cells. Cells were grown in fresh Ham's F12 nutrient medium until cells achieved confluency (passage 1). The cells were split again (using 0.05% trypsin); this cycle was repeated for a total of four passages. On the fifth splitting, cells were plated onto either collagen-coated stretch plates (57.75 cm<sup>2</sup> area per plate; FlexCell International, Hillsborough, NC) or collagen-coated stage-flexer membranes in 10 cm diameter petri plates (FlexCell).

***Stretch-induced cytosolic calcium concentration ( $[Ca^{++}]_i$ ).***

Primary urothelial cells were plated on stage-flexer membranes as described above and incubated in supplemented Ham's F12 growth medium overnight, to 50% confluency. The medium was replaced with Hank's minimal salt medium with calcium added to a final concentration of 1.5 mM. After 1-hour incubation, 5 μM Fura-2 AM (methyl ester) was added and cells were loaded for 30 minutes. The medium was then replaced with Hank's (1.5 mM Ca<sup>++</sup>) and the cells were incubated at 37°C for 1 hour to allow cleavage of the methyl ester and generation of free fura-2 within the cytoplasm.



After Fura-2 loading, the membranes (containing attached urothelial cells at 50% confluency) were removed from petri plates and placed in the Stage-Flexer (Flexcell) apparatus for calcium imaging. 100  $\mu$ l of Hanks (1.5 mM  $\text{Ca}^{++}$ ) was placed onto the cells and the cells were covered with a glass cover slip. The Stageflexer was inverted to place the cover slip side nearest the objective and fixed into place on the stage. Individual cells were identified on 20X objective such that 15-30 cells per field were visible. Fluorescence intensity was measured using intensified CCD dual excitation wavelengths of 340 and 380 nm. To maximize signal and diminish bleaching, a neutral density two filter, 400 nm dichroic mirror, and a 510-nm long-pass emission filter were in place during excitation. (Checura and Parrish, 2006) Neutral Absorbance was measured and electronic images were taken every five seconds. After the resting images were taken, the cells were stretched using the Flexcell apparatus to 20% increase in cell surface size. A maximal 20% increase in surface area is equivalent to the increase in luminal surface area observed during intraluminal ureteral pressures of 46 mm Hg. (Flexcell Manual) Excitation and imaging were performed every five seconds for five minutes. After this time, stretch was removed and excitation and imaging were continued at five-second intervals for one minute after returning the cells to the resting phase.

$[\text{Ca}^{++}]_i$  at all time points was determined by the formula:

$$\text{Eq.1:} \quad [\text{Ca}^{++}]_i = K_d \left[ \frac{(R - R_{\min})}{(R_{\max} - R)} \right] \left[ \frac{F_{\max}^{380}}{F_{\min}^{380}} \right]$$

where  $K_d$  is binding affinity of Fura-2 to calcium,  $R$  is the observed intensity value for each cell,  $R_{\min}$  is the 340/380 ratio in calcium-free medium,  $R_{\max}$  is 340/380 in 1 mM calcium,  $(F_{\max}^{380}/F_{\min}^{380})$  is the emission at 510 nm in 1 mM  $Ca^{++}$  medium/ $Ca^{++}$  free medium. In our system,  $Ratio_{\min}=0.48$ ,  $Ratio_{\max}=11$ ,  $K_d=225$ , and  $F_{\max}^{380}/F_{\min}^{380}=10$ .

To test the repeatability and durability of the calcium response, the above methodology was repeated three times, and  $[Ca^{++}]_i$  measured and compared for each repeated stimulus. In addition, a separate subset of cells was stretched with 20% cyclic stretch (12 cycles per minute) for 1 hour, and the above calcium concentration methodology was applied to the cells to determine the calcium response after 1 hour of cyclic stretch.

### ***The effect of calcium chelation on stretch-induced COX-2 expression***

Primary urothelial cells were plated on 6-well Bioflex (Flexcell Int.) tissue culture plates as described above and incubated in supplemented Ham's F12 growth medium overnight, to 80-90% confluency. The cells were incubated with supplemented Ham's F12 containing 0.3, 1, 3, 10, 30, or 100  $\mu$ M BAPTA-AM or 0.1% DMSO (vehicle) for 30 minutes. The plates were placed on the cell stretch apparatus (FX-3000T; FlexCell); version 3.2 Tension Plus software was used to control the apparatus. Tension (stretch) was applied to the bottom of the flexible stretch membranes by pressure driven posts, controlled by the software. We stretched the cells to 20% increase in cell surface area using cyclic stretch at a rate of 12 cycles per minute for 6 hours, as this was previously determined to produce optimal induction of COX-2 expression. (Jerde et al, 2006) Unstretched cells were used as controls.

After conclusion of the 6-hour stretch period, protein collections were assayed for COX-2 and GAPDH protein by immunoblotting. Cells were collected in protease inhibitor containing lysis buffer (150 mM NaCl, 10 mM Tris, 1 mM EDTA, 1mM phenylmethylsulfonyl flouride, and 10 µg/ml each of leupeptin, aprotinin, and antipain [Sigma]). Triton X-100 was added to a concentration of 1.0% and the homogenate was incubated for 30 minutes at 4°C, followed by centrifugation for 10 minutes at 14,100xG. The protein collections (20 µg/well) were resolved by electrophoresis in 10% SDS-PAGE gel. Proteins were transferred to nitrocellulose blotting membranes, blocked overnight in blotto B + azide [10 g/L nonfat dry milk, 10 g/L bovine serum albumin, 0.5 g/L NaN<sub>3</sub> in 1X phosphate-buffered saline (PBS: 2.7 mM KCl, 1.5 mM KH<sub>2</sub>PO<sub>4</sub>, 136 mM NaCl, 8 mM Na<sub>2</sub>HPO<sub>4</sub>) + 0.05% (v/v) tween 20] and incubated with either mouse monoclonal anti-COX-2 (18 hours, Cayman Chemical, Ann Arbor, MI), or mouse monoclonal anti-GAPDH (1 hour, Abcam, Poole, UK) diluted in blotto B + azide. After washing in PBS+ 0.05% tween-20, the blots were incubated with either goat anti-mouse or goat anti-rabbit IgGs conjugated to horseradish peroxidase for 1 hour (Pierce, Rockford, IL) in blotto B (50 g/L nonfat dry milk, 20 g/L BSA in PBS+0.05% tween 20). Peroxidase activity was detected via West Femto chemiluminescence reagent as directed by the manufacturer (Pierce). Photoimages were analyzed by NIH image Scion software for densitometry, and ratios of COX-2 to GAPDH were determined and compared between obstructed and normal ureter. Statistical evaluation was calculated with unpaired student t-test (obstructed versus normal), and data are presented as mean (± standard deviation) with corresponding p-values.

To determine if simple calcium induction would reciprocally induce COX-2 induction, we treated additional cells with 1 and 10 µM concentrations of 4-bromo-calcium ionophore for 6

hours and measured COX-2 protein expression by immunoblotting, in the presence and absence of cell stretch.

### ***Stretch-induced protein kinase C activation***

Primary urothelial cells were plated in 6-well Bioflex collagen-coated tissue culture plates as described above and incubated in supplemented Ham's F12 growth medium overnight, to 80-90% confluency. To determine the presence of PKC isoforms, cells were stretched for 30, 45, 60, 90 or 120 minutes and immunoblotted for PKC  $\alpha$ ,  $\beta$ 1,  $\beta$ 2,  $\gamma$ ,  $\delta$ ,  $\epsilon$ ,  $\theta$ ,  $\eta$ ,  $\lambda/\iota$ , and  $\zeta$  isoforms. It was determined that human urothelial cells highly expressed PKC $\alpha$ ,  $\beta$ 1, and  $\zeta$ , exhibited little expression of  $\delta$ ,  $\epsilon$ ,  $\eta$ , and  $\lambda/\iota$  and  $\beta$ 2,  $\gamma$ , and  $\theta$  were undetectable. It was also determined that PKC $\alpha$ ,  $\beta$ 1, and  $\zeta$  were down regulated beyond 60 minutes of stretch. Based on these preliminary findings, we sought to determine the activation of PKC $\alpha$ ,  $\beta$ 1, and  $\zeta$  by measuring translocation to plasma membrane and nucleus after 45 minutes of stretch. For all experiments, unstretched cells and cells treated with 1  $\mu$ M phorbol myristyl acetate (phorbol ester, PMA) were used as negative and positive controls, respectively.

To isolate the plasma membrane, we stretched 4, 6-well plates (approximately  $10^8$  cells) as described, washed once with PBS, and collected them in TEDK (10 mM Tris-HCl (pH 7.2), 0.3M KCl, 1mM EDTA, 5 mM DTT+1x protease inhibitor cocktail) with a cell scraper. We homogenized the cells with 40 strokes of a Dounce homogenizer, centrifuged the suspension at 500G for 10 minutes to pellet the nuclei, and collected the supernatant. The supernatant was centrifuged 27,000xG for 30 minutes to collect membrane and organelles. The resulting pellet was

resuspended in 2 ml TEDK plus 15% sucrose and layered over a sucrose gradient of 30% sucrose in TEDK over 45%. The gradient was centrifuged at 76,000xG for 3 hours to separate the membrane fraction from the organelles. The 15-30% interface was collected in TEDK and centrifuged at 100,000xG for 1 hour. The pellet was resuspended in TEDK as the membrane fraction. (Bermudez-Rivera et al, 2002)

To isolate the cytosol, we stretched 1, 6-well plate (approximately  $10^7$  cells) as described, washed once with PBS, and collected them in TEDK with a cell scraper. We homogenized the cells with 40 strokes of a Dounce homogenizer, centrifuged the suspension at 500xG for 10 minutes to pellet the nuclei, and collected the supernatant. The plasma membrane and nuclei were pelleted by centrifugation at 100,000xG for 1 hour. The supernatant was collected as the cytosolic fraction. (Bermudez-Rivera et al, 2002)

To isolate the nuclei, we stretched 3, 6-well plates (approximately  $5 \times 10^7$  cells) as described, washed once with buffer A (10 mM Tris base [pH=7.8], 5 mM MgCl<sub>2</sub>, 10 mM KCl, 0.3 mM EGTA, 0.3 mM sucrose, 10 mM  $\beta$ -glycerophosphate, 1 mM phenylmethylsulfonyl fluoride, 0.5 mM DTT, 1% protease inhibitor cocktail), and collected them in buffer A with a cell scraper. After placing the cells on ice for 15 minutes, the cells were lysed with Nonidet P40 at a final concentration of 0.6% and vortexing for 20 seconds at highest speed. The suspension was centrifuged at 7200xG for 2 minutes to pellet the nuclei, and the pellet was resuspended in 300  $\mu$ l of buffer B (20 mM Tris base [pH=7.8], 5 mM MgCl<sub>2</sub>, 320 mM KCl, 0.5 mM DTT, 1% protease inhibitor cocktail). This suspension was incubated on ice for 15 minutes to disrupt the nuclei and solubilize the proteins. The suspension was centrifuged at 13,500xG for

15 minutes and the supernatant was collected as the nuclear extract. (Bermudez-Rivera et al, 2002)

Protein extracts from all three fractions were quantified and immunoblotted for PKC isoforms  $\alpha$ ,  $\beta$ 1, and  $\zeta$ . Fraction purity for cytosolic and nuclear protein extraction was assessed by immunoblotting each fraction for lactate dehydrogenase (exclusively cytosolic protein) and nuclear lamin B1 (exclusively nuclear protein) using the immunoblotting methods described. Plasma membrane fraction purity was assessed by assaying each fraction for adenylyl cyclase activity (exclusively plasma membrane protein) using an activity assay (Molecular Devices, Sunnyvale, CA) in which protein extract from each fraction was assessed for its ability to generate cAMP from ATP in conditions recommended by the manufacturer.

### ***The effect of Protein kinase C inhibition on stretch-induced COX-2 expression***

Primary urothelial cells were plated on 6-well Bioflex tissue culture plates as described above and incubated in supplemented Ham's F12 growth medium overnight, to 80-90% confluency. The cells were incubated with supplemented Ham's F12 containing 1, 10, or 100 nM bisindolylmaleimide-1; 3, 10, or 30  $\mu$ M myristylated PKC pseudosubstrate peptide, or 0.1% DMSO (vehicle) for 1 at a rate of 12 cycles per minute for 6 hours, as previously described. Unstretched cells were used as controls. After conclusion of the 6-hour stretch period, protein collections were assayed for COX-2 and GAPDH protein by immunoblotting.

Additional primary urothelial cells were plated on 6-well Bioflex tissue culture plates as described above and incubated in supplemented Ham's F12 growth medium overnight, to approximately 60% confluency. Oligofectamine<sup>TM</sup>-siRNA complexes were generated for 30 minutes in OPTI-MEM<sup>TM</sup> medium in conditions recommended by the manufacturer (Invitrogen, Carlsbad, CA) using 23 base siRNA sequences (Dharmacon, Lafayette, CO) directed against PKC $\alpha$ , PKC $\beta$ 1, or PKC $\zeta$ . The complexes were added to the cells in supplemented Ham's F12 such that the final dilution in the wells was 10  $\mu$ l Oligofectamine<sup>TM</sup> per ml of medium and either 250 nM PKC $\alpha$  siRNA, 500 nM PKC $\beta$ 1siRNA, or 500 nM PKC $\zeta$  siRNA. These were the transfection conditions determined to be optimal in preliminary experiments. The transfections were allowed to progress for 48 hours; this time point was determined to be optimal in preliminary experiments. Additional cells were transfected with negative control RNA previously shown to not silence any gene in the human genome (Dharmacon), and untransfected cells were used as a second negative control. After the 48-hour transfection period, the cells were harvested and protein extracts were immunoblotted for GAPDH, COX-2, PKC $\alpha$ , PKC $\beta$ 1, and PKC $\zeta$ , as described above. PKC expression knockdown was determined by measuring densitometry of each PKC band relative to its GAPDH loading control and compare this to cells transfected with negative control RNA.

**siRNA controls:** To determine the effect of siRNA transfection and reagents on COX-2 and PKC expression in urothelial cells, preliminary experiments were performed in which stretched and unstretched urothelial cells were transfected with unrelated siRNA controls with Oligofectamine, treated with Oligofectamine alone, or untreated. No effect of nonsense siRNA transfection or Oligofectamine was observed, and inducibility of COX-2 was unaffected.

### *Calcium dependence of PKC $\zeta$ activation*

In order to examine the interrelationship of the critical PKC isoform and calcium in stretch-induced COX-2 induction, we sought to determine if PKC $\zeta$  activation was dependent on calcium. First, activation of the zeta isoform of PKC was determined by phosphorylation of threonine residues 403 and 410, by phospho-specific antibody (Abcam). Cells were stretched for 0.5, 1, 2, and 4 hours with 20% cyclic stretch (12 cycles per minute), total cell protein extract was collected, and phosphorylation of PKC $\zeta$  was determined by immunoblotting. After confirming that optimal induction occurred within 2 hours of stretch, cells were incubated with supplemented Ham's F12 containing 3, 10, or 30  $\mu$ M BAPTA-AM or 0.1% DMSO (vehicle) for 30 minutes. Cells were stretched for 1 hour with 20% cyclic stretch (12 cycles per minute), and total cell protein extract was collected in the presence of protease and phosphatase inhibitors. Immunoblotting for phospho-(Thr 403/410) PKC $\zeta$  activation was determined by immunoblotting by phospho-specific antibody.



## **RESULTS**

### ***The effect of stretch on $[Ca^{++}]_i$ :***

Panels A through D [**Figure 1**] show individual cell fields after various times of stretch applied to resting cells (Panel A) with the color intensity relating to changes in  $[Ca^{++}]_i$  such that the range of blue to white represent low to high levels. The average values of multiple individual cell fields (n=5) of  $[Ca^{++}]_i$  is represented in Panel F [**Figure 1**] and demonstrates that  $[Ca^{++}]_i$  increased from 44 nM in resting cells to 430 nM after 30 seconds of 20% stretch. After 60 seconds of stretch,  $[Ca^{++}]_i$  began to gradually decrease throughout the 5 minute stretch period, to an average of 210 nM. All measured differences in cells stretched to 20% and 10% were statistically significant above unstretched controls at all time points of stretching, as determined by unpaired student's T-test, p-values <0.01. In addition, 20% stretch produced statistically significant increase compared to 10% stretch after 15 seconds of stretch, continuing throughout the stretch. Upon removing stretch from the cells, a second transient increase in  $[Ca^{++}]_i$  occurred, to a maximal point of 405 nM. This second increase lasted approximately 10 seconds before a rapid decrease that reduced  $[Ca^{++}]_i$  to an average of 62 nM. No statistical difference was noted in calcium induction induced by removing 20% stretch and 10% stretch. The rapid induction of  $[Ca^{++}]_i$  was repeatable within each experiment, as the cells could be induced to concentrations of  $[Ca^{++}]_i$  greater than 400 nM at least 3 times in succession. Similarly, cells stretched for 1 hour prior to calcium measurements had responsiveness similar to previously unstretched cells, as all cells were inducible to greater than 400 nM  $[Ca^{++}]_i$ . Positive control cells treated with 10  $\mu$ M 4-bromo-calcium ionophore exhibited  $[Ca^{++}]_i$  of 962 nM after 60 seconds of treatment.

***The effect of calcium chelation on stretch-induced COX-2 expression:***

Stretch induced an 8-fold increase in COX-2 protein content compared to non-stretched controls (the ratio of COX-2 to GAPDH was 1.26 (+/- 0.15) in stretched cells and 0.16 (+/- 0.04) in control cells (n=6, p=0.001) [Figure 2A]. Calcium chelation with BAPTA-AM reduced this induction in a dose-manner such that the ratio of COX-2 to GAPDH was 0.54 in 1  $\mu$ M BAPTA-AM-treated stretched cells, 0.15 in 3  $\mu$ M BAPTA-AM-treated stretched cells, 0.06 in 30 $\mu$ M BAPTA-AM-treated stretched cells and 0.07 in 100  $\mu$ M BAPTA-AM-treated cells. All four concentrations studied produced statistical significance relative to vehicle (DMSO) treated control cells, student's T-Test p<0.01. The highest concentration of calcium chelation also reduced the expression of COX-2 in unstretched cells, as the ratio of COX-2 to GAPDH was reduced from 0.16 in untreated unstretched cells to 0.06 with 100  $\mu$ M BAPTA-AM treatment. This was the only concentration of BAPTA-AM to exhibit significant inhibition in unstretched cells (p=0.02).

To determine if induction of calcium flux alone was sufficient to induce COX-2 expression, we treated stretched and unstretched cells with 4-bromo-calcium ionophore for 6 hours. Induction of calcium flux with 1  $\mu$ M ionophore induces COX-2 expression 8-fold in unstretched cells. (Figure 2B) Addition of 10  $\mu$ M ionophore had only a marginal increase above 1  $\mu$ M. Addition of ionophore to stretched cells doubled the expression of COX-2; however this induction was equal to that of ionophore alone, suggesting that calcium flux and stretch induce COX-2 via a similar mechanism.

***The effect of stretch on PKC translocation:***

In preliminary experiments, we determined that stretched and unstretched human urothelial cells expressed protein kinase C (PKC)  $\alpha$ ,  $\beta_1$ , and  $\zeta$  isoforms. No presence of  $\beta_2$ ,  $\gamma$ ,  $\eta$ , and  $\theta$  were observed and only weak presence of  $\delta$ ,  $\epsilon$  and  $\lambda/\iota$  were identified [Data not shown]. Stretched cells exhibited marked translocation of PKC  $\alpha$ ,  $\beta_1$  and  $\zeta$  to the plasma membrane and nucleus, indicating activation. **[Figure 3]** For PKC $\alpha$ , urothelial cells stretched for 45 minutes exhibited a plasma membrane to cytosol (m/c) ratio of 2.7 and a nucleus to cytosol (n/c) ratio of 3.1 compared to a m/c ratio of 0.16 (p=0.007) and a n/c ratio of 0.13 (p=0.03) in unstretched cells (n=4). For PKC $\beta_1$  stretched cells exhibited an m/c ratio of 6.9 and a nucleus to cytosol (n/c) ratio of 6.3 compared to an m/c ratio of 0.07 (p=0.02) and an n/c ratio of 0.06 (p=0.002) in unstretched cells (n=4). For PKC $\zeta$ , stretched cells exhibited an m/c ratio of 8.8 and a n/c ratio of 9.0 compared to an m/c ratio of 1.1 (p=0.04) and an n/c ratio of 1.1 (p=0.02) in non-stretched cells (n=4). Phorbol ester induced translocation of PKC $\alpha$  (m/c: p=0.02; n/c: p=0.03) and  $\beta_1$  (m/c: p=0.01; n/c: p=0.003) but not  $\zeta$  (m/c: p=0.80; n/c: p=0.85). We verified cell fraction purity by blotting for lactate dehydrogenase (a cytosolic protein) and nuclear lamin B1 (a nuclear protein), and assessing adenylyl cyclase activity (plasma membrane protein). These data indicate that PKC is activated and translocated to the plasma membrane and nuclear region during cell stretch.

***The effect of pharmacologic PKC inhibition on stretch-induced COX-2 expression:***

In untreated cells, the ratio of COX-2 to GAPDH was 1.20 in stretched cells and 0.12 (n=6, p=0.001) in control cells. **[Figure 4-5]** Pharmacologic PKC inhibition with bisindolylmaleimide-1 reduced COX-2 induction in a concentration-dependent manner. COX-2 to GAPDH ratios were 0.92, 0.22 (p=0.001), and 0.13 (p=0.005) in 1, 10, and 100 nM bisindolylmaleimide-1-treated stretched cells, respectively (n=6, **Figure 4**). Similarly, COX-2 to GAPDH ratios were 0.80, 0.32 (p=0.006), and 0.30 (p=0.01) in 3, 10, and 30  $\mu$ M PKC pseudosubstrate peptide-treated stretch-induced cells, respectively **[Figure 5]**. Neither PKC inhibitor reduced COX-2 expression significantly from untreated controls in unstretched cells.

***The effect of PKC $\alpha$ ,  $\beta$ 1, and  $\zeta$  RNA interference on stretch-induced COX-2 expression:***

Transfection of urothelial cells with siRNA directed against PKC $\alpha$  reduced PKC $\alpha$  expression by 91%. In these cells, the COX-2 to GAPDH ratio was slightly reduced from 1.0 in stretched control siRNA transfected cells to 0.79 in PKC $\alpha$  RNAi transfectants. **[Figure 6]** However, this reduction was not statistically significant, though a clear trend was present (p=0.06, n=4). Transfection of cells with siRNA directed against PKC $\beta$ 1 reduced PKC $\beta$ 1 expression by 60%. This had no significant effect on stretch-induced COX-2 expression. However, unstretched cells transfected with siRNA directed against PKC $\beta$ 1 exhibited a slight, statistically insignificant trend of increased COX-2 expression compared to non-transfected unstretched controls (n=4, p=0.08). **[Figure 6]** Transfection of urothelial cells with siRNA directed against PKC $\zeta$  inhibited PKC $\zeta$  expression by 71%. The COX-2 to GAPDH ratio was significantly reduced from 1.0 in stretched siRNA control cells to 0.32 in PKC $\zeta$  RNAi transfectants (p=0.005, n=4). **[Figure 6]**

### *Calcium dependence of PKC $\zeta$ activation*

To determine the dependence of PKC $\zeta$  induction on calcium signaling, we pretreated urothelial cells with BAPTA-AM for 30 minutes prior to stretching. We then analyzed cellular protein for PKC $\zeta$  phosphorylation (a marker of PKC $\zeta$  activation) by immunoblotting with phospho-specific antibodies. Stretch of urothelial cells for two hours induced the phosphorylation of PKC $\zeta$  3-fold, indicating activation. Chelation of intracytosolic calcium with BAPTA attenuated this response, as 30  $\mu$ M BAPTA-AM reduced PO<sub>4</sub>-PKC $\zeta$  to unstretched levels. The data shown are the ratio of PO<sub>4</sub>-PKC $\zeta$  to GAPDH quantified from three cell lines (n=3) in duplicate. Total PKC $\zeta$  levels did not change in this experiment, indicating phosphorylation and activation processes are involved in PO<sub>4</sub>-PKC $\zeta$  increase rather than induction of PKC $\zeta$  expression.

## DISCUSSION

Our data indicate that calcium and PKC $\alpha$ ,  $\beta$ 1, and  $\zeta$  are induced by cell stretch in primary human urothelial cells. In addition, our data indicate that calcium and PKC $\zeta$  are necessary for COX-2 expression in this model, and suggest that PKC $\alpha$  may play a secondary role. This is the first report specifically linking PKC $\zeta$  to mechanically induced COX-2 expression. While other studies have used pharmacologic inhibitors to determine that PKC isoforms are involved in mechanotransduction involving vascular endothelial cells, and bone cells, this is the first study that we are aware of that uses siRNA targeting to specifically silence expression of the PKC $\zeta$  isoform. This is also the first report to illustrate specific PKC isoform activation in response to cell stretch. Although PKC $\zeta$  has been implicated in COX-2 induction in overexpression studies (Miller et al, 1997), this is the first report identifying calcium and PKC as being integral to stretch-induced COX-2 expression in urothelial cells, the primary prostaglandin producing cells in the urinary tract, particularly as it relates to the pathophysiology of ureteral obstruction. (Ali et al, 1998)

Our previous work illustrates the reproducibility and reliability of the urothelial cell model in relation to in vitro ureteral obstruction. In addition, Park and associates have demonstrated similar reproducibility using a bladder smooth muscle cell model and in vivo distended detrusor. (Park et al, 1997) Still, the calcium flux associated with rapidly inducible cell stretch produced in vitro may not correlate temporally or quantitatively with what is actually occurring in vivo. Our cell culture model has shown a more rapid induction of gene expression than what is observed in our in vivo obstruction model. Similarly, it is possible that differential

PKC expression *in vitro* could distort the overall importance of each PKC isoform as it relates to their contribution to *in vivo* mechanotransduction in general, and distension-induced COX-2 expression in particular. New isoform selective PKC inhibitors are in development, and inducible gene knockout animal models may allow for assessment of selective isoform inhibition *in vivo*.

We did not expect PKC $\zeta$  to be the primary isoform of PKC involved in stretch-induced COX-2 expression, and it was even more unexpected that PKC $\alpha$  would have such a minimal effect. Our data clearly show the dependence of COX-2 induction on calcium, yet PKC $\zeta$  is a calcium-independent isoform of PKC. Our data show that PKC $\zeta$  activation, as measured by phosphorylation, is dependent upon available calcium in our system. However, the questions of how and to what extent PKC $\zeta$  might be dependent on calcium in cell biology are unresolved in by our study, and were not the intent of our study. This effect could be direct or indirect, and future work will be directed at answering these important questions. While little is known regarding PKC $\zeta$  activation, there is evidence that phosphoinositide-dependent kinase (PDK)-1 phosphorylates and activates PKC $\zeta$  secondary to phosphoinositol triphosphate kinase (PI<sub>3</sub>K) signaling. (Hirai et al, 2003) Recent evidence from bone cells indicates this is a calcium driven process, (Danciu et al, 2003) but the role calcium plays in this process is not clear. It is feasible that the role of calcium in PDK-1 activation and the role of the calcium and classical PKC isoforms in our model are related, and some level of cross talk between the classical and atypical PKC isoforms may occur during urothelial cell stretch. Classical PKC isoforms and PKC $\zeta$  have been shown to cross talk in NIH3T3 cells induced with phorbol ester. (Kim et al, 1997) While we found no effect of PKC $\beta$ 1 knockdown on stretch-induced COX-2 expression, PKC $\beta$ 1 may compensate for the lack of PKC $\alpha$  activity the presence of PKC $\alpha$  knockdown. Future studies

should be directed toward evaluating these hypotheses with COX-2 expression and PKC $\zeta$  activation studies in the presence of calcium chelation, PKC $\alpha$ /PKC $\beta$ 1 double knockouts, and PI $_3$  kinase inhibitors. Finally, while siRNA knockdown of whole cell PKC $\alpha$  or  $\beta$ 1 protein give inconclusive results, these data do not yet consider any differences in nuclear or plasma membrane localization of these isoforms. It is possible that, even with 91% and 62% knockdown of PKC $\alpha$  and  $\beta$ 1 respectively, there still could be a significant concentration of activated kinase in the nuclear or plasma membrane. Future studies evaluating the cellular localization of the PKC isoforms during RNA interference should be performed.

Calcium and PKC may induce COX-2 in response to cell stretch via several known pathways. Many signaling cascades of COX-2 induction have been identified, including those involving MAP kinases, PI $_3$ K-Akt, nuclear factor kappa-B (NF $\kappa$ B), steroid hormone receptors, and extracellular matrix proteins, all which may be modulated by calcium and PKC. (Santen et al, 2002; Appleby et al, 1994; Yamamoto et al, 1995; Tamura et al, 2002; Di Mari et al, 2003) However, most of these studies involved hormone or mitogen-induced conditions and data investigating mechanosensing pathways of COX-2 induction remain sparse. Stretch-induced COX-2 expression in bladder smooth muscle, renal podocytes, and osteoblasts does appear to be mitogen-activated protein (MAP) kinase-dependent, especially with regard to p38. (Fitzgerald et al, 2004; Martineau et al, 2004; Naruse et al, 2003) In addition, deletion analysis of COX-2 promoter elements has determined the importance of C/EBP $\beta$ , CRE, and AP-1 elements in shear stress-induced COX-2 expression in murine osteoblasts. (Ogasawara et al, 2001) However, the triggering cascades of these molecules are yet to be determined in mechanically stimulated cells. The cellular mechanisms by which stretch induces COX-2 expression are an active area of



investigation, and will likely lead to pharmacologic targets of intervention for stretch and pressure-related diseases.

## **ACKNOWLEDGEMENTS**

The authors gratefully acknowledge Abdullah Kaya, PhD, for expert assistance in operating the fluorescent imaging microscope, Glen Leverson, PhD, for statistical analysis of the data, Paul Bertics, PhD, for insightful discussions of the data, and Nicholas Weber for imaging analysis and manuscript preparation.

## REFERENCES

Ali M, Angelo-Khattar M, Thulesius L, Fareed A, Thulesius O (1998) Urothelial synthesis of prostanoids in the ovine ureter. *Urol Res.* **26 (3)**:171-174.

Appleby SB, Ristimaki A, Neilson K, Narko K, Hla T (1994) Structure of the human cyclooxygenase-2 gene. *Biochem. J.* **302 (3)**: 723-727.

Basar I, Bircan K, Tasar C, Ergen A, Cakmak F, Remzi D (1991) Diclofenac sodium and spasmolytic drugs in the treatment of ureteral colic: a comparative study. *Int Urol Nephrol.*; **23(3)**: 227-230.

Brune K, Neubert A (2001) Pharmacokinetic and pharmacodynamic aspects of the ideal COX-2 inhibitor: a pharmacologist's perspective. *Clinical & Experimental Rheumatology.* **19(6)**: S51-57.

Checura CM, Parrish JJ, (2006) The role of calcium in maturation and activation of horse oocytes. *An. Reprod. Sci.* **94**: 340-342.

Chou SY, Cai H, Pai D, Mansour M, Huynh P (2003) Regional expression of cyclooxygenase isoforms in the rat kidney in complete unilateral ureteral obstruction. *J. Urol*, **170**: 1403-1408.

Clark JY, Thompson IM, Optenberg SA (1995) Economic impact of urolithiasis in the United States. *J. Urol.* **154**: 2020-2024.

Cole RS, Fry CH, Shuttleworth KE (1988) The action of the prostaglandins on isolated human ureteric smooth muscle. *Br J Urol.*; **61(1)**:19-26.

Colletti AE, Vogl HW, Rahe T, Zambraski EJ (1999) Effects of acetaminophen and ibuprofen on renal function in anesthetized normal and sodium-depleted dogs. *J. Appl Physiol.* **86(2)**: 592-597.

Danciu TE, Adam RM, Naruse K, Freeman MR, Hauschka PV (2003) Calcium Regulates the PI3K-Akt pathway in stretched osteoblasts. *FEBS Letters* **536**: 193-197.

Di Mari JF, Mifflin RC, Adegboyega PA, Saada JI, Powell DW (2003) IL-1 $\alpha$ -induced COX-2 expression in human intestinal myofibroblasts is dependent on a PKC $\zeta$ -ROS pathway. *Gastroenterology*, **124**: 1855-1865.

Fitzgerald JB, Jin M, Dean D, Wood DJ, Zheng MH, Grodzinsky AJ (2004) Mechanical compression of cartilage explants induces multiple time-dependent gene expression patterns and involves intracellular calcium and cyclic AMP. *J Biol Chem.* **279(19)**:19502-19511.

Foegh ML, Hecker M, Ramwell PW (1999) The eicosanoids: Prostaglandins, thromboxanes, leukotrienes and related compounds. In Basic and Clinical Pharmacology, Katzung BG, ed. McGraw-Hill, New York, NY.

Gulmi FA, Felson D, Vaughan ED (1998) Physiology of ureteral obstruction. In Campbell's Urology. Walsh PC, Retik AB, Vaughan ED, Wein A eds. Chapter 9- pp.324-379, WB Saunders, Philadelphia, PA.

Hamill OP, and Martinac B (2001) Molecular basis of mechanotransduction in living cells. *Physiol. Rev.* **81(2)**: 685-740.

Hernandez J, Astudillo H, Escalante B (2002) Angiotensin II stimulates cyclooxygenase-2 mRNA expression in renal tissue from rats with kidney failure. *Am J Physiol-Renal Physiol.* **282(4)**: F592-598.

Hirai T, Chida K (2003) Protein kinase C zeta (PKC zeta): activation mechanisms and cellular functions. *J. Biochem.* **133(1)**: 1-7.

Inoue H, Taba Y, Miwa Y, Yokota C, Miyagi M, Sasaguri T (2002) Transcriptional and posttranscriptional regulation of cyclooxygenase-2 expression by fluid shear stress in vascular endothelial cells. *Arterioscler Thromb Vasc Biol.* **22(9)**: 1415-1420.

Jerde TJ, Mellon WS, Bjorling DE, Nakada SY (2006) Evaluation of urothelial stretch-induced cyclooxygenase-2 expression in novel human cell culture and porcine in vivo ureteral obstruction models. *J Pharmacol Exp Ther.* **317(3)**: 965-972

Kim SJ, Chang YY, Kang SS, Chun SJ (1997) Phorbol Ester Effects In Atypical Protein Kinase C  $\zeta$  Overexpressing NIH3T3 Cells: Possible Evidence For Crosstalk Between Protein Kinase C Isoforms. *Biochem Biophys Res Comm.* **237**: 336-339.

Kujuba DA, Fletcher BS, Varnum BC, Lim RW, Herschmann HR (1991) TIS10, a phorbol ester tumor-promoter-inducible mRNA from Swiss 3T3 cells, encodes a novel prostaglandin synthase/cyclooxygenase homologue. *J. Biol. Chem.* **266**: 12866-12872.

Lanza GL, Rack MF, Simon TJ, Quan H, Bolognese JA, Hoover ME, Wilson FR, Harper SE (1999) Specific inhibition of cyclooxygenase-2 with MK-0966 is associated with less gastroduodenal damage than either aspirin or ibuprofen. *Aliment. Pharmacol. Ther.* **13(7)**: 761-767.

Malhotra A, Kang BP, Opawumi D, Belizaire W, Meggs LG. (2001) Molecular biology of protein kinase C signaling in cardiac myocytes. *Mol. Cell. Biochem.* **225(1)**: 97-107.

Martineau LC, McVeigh LI, Jasmin BJ, Kennedy CR. (2004) p38 MAP kinase mediates mechanically induced COX-2 and PG EP4 receptor expression in podocytes: implications for the actin cytoskeleton. *Am J Physiol-Renal Physiol.* **286(4)**: F693-701.

Miller BW, Baier LD, Morrison AR (1997) Overexpression of protein kinase C-zeta isoform increases cyclooxygenase-2 and inducible nitric oxide synthase. *Am. J. Physiol.* **273**: C130-136.

Mukherjee D, Nissen SE, Topol, EJ (2001) Risk of cardiovascular events associated with selective COX-2 inhibitors. *JAMA.* **286(8)**: 954-959.

Nakada SY, Jerde TJ, Jacobson LM, Saban R, Bjorling DE, Hullett DA (2002) Cyclooxygenase-2 expression is upregulated in obstructed human ureter. *J. Urol.* **168**: 1226-1229.

Naruse K, Miyauchi A, Itoman M, Mikuni-Takagaki Y (2003) Distinct anabolic response of osteoblast to low-intensity pulsed ultrasound. *J Bone Miner Res.* **18(2)**: 360-369.

Newton AC (1995) Protein Kinase C: Structure, Function, and Regulation. *J. Biol. Chem.* **270**: 28495-28498.

Ogasawara A, Arakawa T, Kaneda T, Takuma T, Sato T, Kaneko H, Kumegawa M, Hakeda Y (2001) Fluid shear stress-induced cyclooxygenase-2 expression is mediated by C/EBP beta, cAMP-response element-binding protein, and AP-1 in osteoblastic MC3T3-E1 cells. *J Biol Chem.* **276(10)**: 7048-7054.

Oren R, Ligumsky M (1994) Indomethacin-induced colonic ulceration and bleeding. *Ann. Pharmacother.* **28**: 883-885.

Park JM, Yang T, Arend LJ, Smart AM, Schnermann JB, Briggs JP (1997) Cyclooxygenase-2 is expressed in bladder during fetal development and stimulated by outlet obstruction. *Am. J. Physiol.* **273(4 Pt 2)**: F538-544.

Ramello A, Vitale C, Marangella M (2000) Epidemiology of nephrolithiasis. *J. Nephrol.* **13(3)**: S65-70.

Rivera-Bermudez MA, Bertics PJ, Albrecht RM, Mosavin R, Mellon WS (2002) 1,25-Dihydroxyvitamin D3 selectively translocates PKC $\alpha$  to nuclei in ROS 17/2.8 cells. *Mol Cell Endocrinol.* **188**: 227-239.

Santen RJ, Song RX, McPherson R, Kumar R, Adam L, Jeng MH, Yue W (2002) The role of mitogen-activated protein (MAP) kinase in breast cancer. *J. Steroid Biochem. Mol. Biol.* **80(2)**: 239-256.

Tamura M, Sebastian S, Gurates B, Yang S, Fang Z, Bulun SE (2002) Vascular endothelial growth factor up-regulates cyclooxygenase-2 expression in human endothelial cells. *J. Clin. Endo. Met.* **87(7)**: 3504-3507.



Taoulllec D, Pianetti P, Coste H, Bellevergue P, Grand-perret T, Ajakane M, Baudet V, Boissing P, Boursier E, Loriolle F, Duhamel L, Charon D, Kirilovsky J (1991) The bisindolylmaleimide GF 109203X is a potent and selective inhibitor of protein kinase C. *J. Biol. Chem.* **266**: 15771-15781.

Teng J, Wang ZY, Bjorling DE (2002) Estrogen-induced proliferation of urothelial cells is modulated by nerve growth factor. *Am. J. Physiol. – Ren. Flu. & Electro. Physiol.* **282(6)**: F1075-1083.

Weiss RM. (1998) Physiology and Pharmacology of the Renal Pelvis and Ureter. In *Campbell's Urology*. (Walsh PC, Retik AB, Vaughan ED, Wein A eds. pp.839-869) WB Saunders, Philadelphia, PA.

Yamamoto K, Arakawa T, Ueda N, Yamamoto S (1995) Transcriptional roles of nuclear factor kappa B and nuclear factor-interleukin-6 in the tumor necrosis factor alpha-dependent induction of cyclooxygenase-2 in MC3T3-E1 cells. *J. Biol. Chem.* **270(52)**: 31315-31320.

## LEGENDS FOR FIGURES

### **Figure 1: Fura-2 ratio (A340/A380) in primary urothelial cells.**

**Panel A** depicts one cell field of unstretched cells, prior to the experiment. **Panel B** depicts cells stretched for 40 seconds while **Panel C** depicts cells stretched for 300 seconds. After stretch was released (**panel D**), a second spike in  $[Ca^{++}]_i$  occurred. **Panel E** is a light-field micrograph of the cells stretched to generate the color images in Panels A-D. **Panel F** depicts the average  $[Ca^{++}]_i$  in stretched urothelial cells as determined by **Eq.1**, 15 determinations per data point, n=5 total cell lines. Maximal induction of calcium was observed at 30 seconds of stretch, after which time  $[Ca^{++}]_i$  gradually decreased. Upon release of stretch, a transient spike in  $[Ca^{++}]_i$  occurred. The average basal  $[Ca^{++}]_i$  was 44 nM while maximal  $[Ca^{++}]_i$  (962 nM) was obtained with 10  $\mu$ M calcium ionophore.

### **Figure 2: Calcium chelation attenuates stretch-induced COX-2 expression, and induction of calcium flux is sufficient to induce COX-2.**

Stretch induced an 8-fold increase in COX-2 protein levels in vehicle (**V**) treated tissues compared to non-stretched controls. Calcium chelation with BAPTA-AM dose-dependently eliminated this induction (**Panel A**; n=5). **Panel B** demonstrates that induction of calcium flux with 4-bromo-calcium ionophore induces COX-2 expression dose-dependently (1, 10  $\mu$ M) in stretched and unstretched urothelial cells. Data in the graph are the ratio of COX-2 expression to GAPDH, the average of 3 cell lines (n=3) performed in duplicate (\*p<0.05, ionophore vs. vehicle).

**Figure 3:** **A.** Blotting for PKC isoforms in cytosol [C], nucleus [N], and membrane [M] with polyclonal antibodies. **B.** Fraction purity was verified by blotting for lactate dehydrogenase and nuclear lamin B1. **C.** Plasma membrane fraction purity was verified by assessment of adenylyl cyclase activity. These data indicate that fractions were pure enough for assessment of PKC translocation.

**Figure 4: Pharmacological PKC inhibition attenuates stretch-induced COX-2 expression.**

**A.** Cell stretch induced COX-2 expression (\*\*\*) $p < 0.001$ - stretched vs. unstretched cells) as shown by quantified data illustrating concentration-dependent attenuation. 10 nM bisindolylmaleimide (Bis) produced statistically significant attenuation ( $\dagger\dagger p < 0.01$ -stretched cells: Bis vs. DMSO vehicle,  $n=6$ ) of stretch-induced COX-2 expression. **B.** Immunoblot illustrating bisindolylmaleimide-attenuation of stretch-induced COX-2 expression.

**Figure 5: Pseudosubstrate PKC inhibition attenuates stretch-induced COX-2 expression.**

**A.** 10  $\mu$ M pseudosubstrate peptide 20-28 (PP 20-28) inhibitor produced statistically significant attenuation of stretch-induced COX-2 expression relative to vehicle-treated cells (DMSO), as illustrated by quantified data from immunoblots ( $\dagger\dagger p < 0.01$ - stretched cells: PP20-28 vs DMSO vehicle,  $n=4$ ). **B.** Immunoblot illustrating the effect of PP 20-28 inhibitor on stretch-induced COX-2 expression.

**Figure 6: siRNA-PKC $\zeta$  transfection attenuates stretch-induced COX-2 expression. A.**

Immunoblots demonstrating PKC isoform specific expression knockdown by specific PKC siRNAs. Expression of PKC $\alpha$ ,  $\beta 1$  and  $\zeta$  in control (non-transfected) cells was compared to that

in PKC $\alpha$ ,  $\beta$ 1, and  $\zeta$  siRNA transfected cells. **B.** Quantified data demonstrates PKC $\zeta$ -siRNA attenuated COX-2 induction. Stretch of cells transfected with control siRNAs or siRNA directed against PKC $\alpha$  or PKC $\beta$  significantly induced COX-2 expression (\* $p < 0.05$ -stretched vs. unstretched control siRNA-treated cells,  $n=4$ ). However, cells transfected with siRNA against PKC $\zeta$  showed significant attenuation of stretch-induced COX-2 expression ( $\dagger\dagger p=0.005$ - PKC $\zeta$  siRNA transfected cells vs. control siRNA transfected cells,  $n=4$ ). PKC $\alpha$  siRNA may have a modulatory effect, though this effect is statistically insignificant with these data sets ( $p=0.21$ ,  $n=4$ ). **C.** Immunoblot illustrating PKC $\zeta$  siRNA attenuation of stretch-induced COX-2 expression.

**Figure 7: Stretch-induced PKC $\zeta$  is dependent upon calcium.** Stretch of urothelial cells induced the phosphorylation of PKC $\zeta$  3-fold, indicating activation (\* $p < 0.05$  (stretched vs. unstretched,  $n=3$ ). Chelation of intracytosolic calcium with BAPTA attenuated this response, as 30  $\mu$ M BAPTA-AM reduced PO $_4$ -PKC $\zeta$  to unstretched levels ( $\dagger p < 0.05$  [0  $\mu$ M vs. 30  $\mu$ M BAPTA-AM],  $n=3$ ). The data shown are the ratio of PO $_4$ -PKC $\zeta$  to GAPDH quantified from three cell lines ( $n=3$ ) in duplicate.

Figure 1; A-E

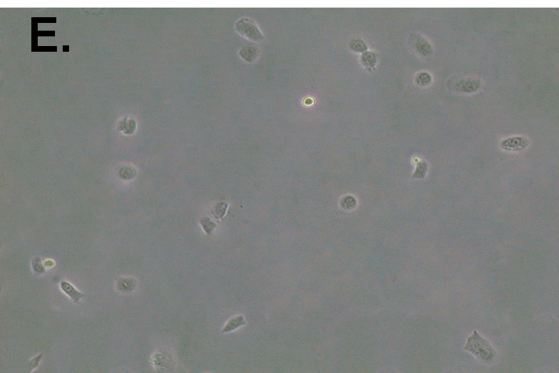
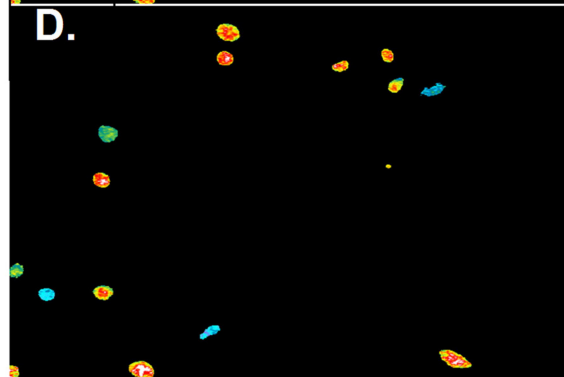
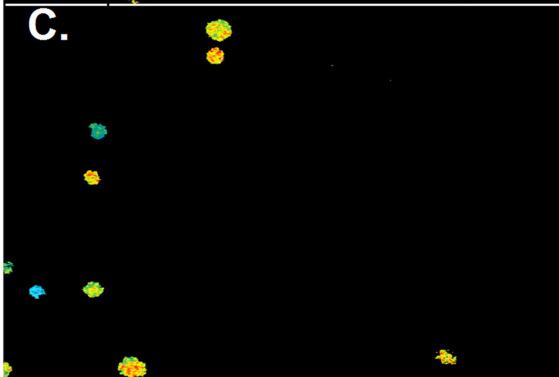
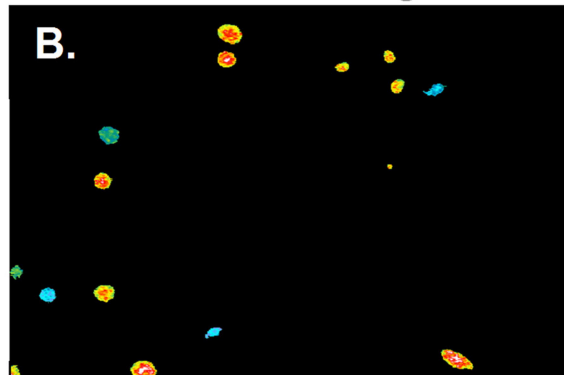


Figure 1F

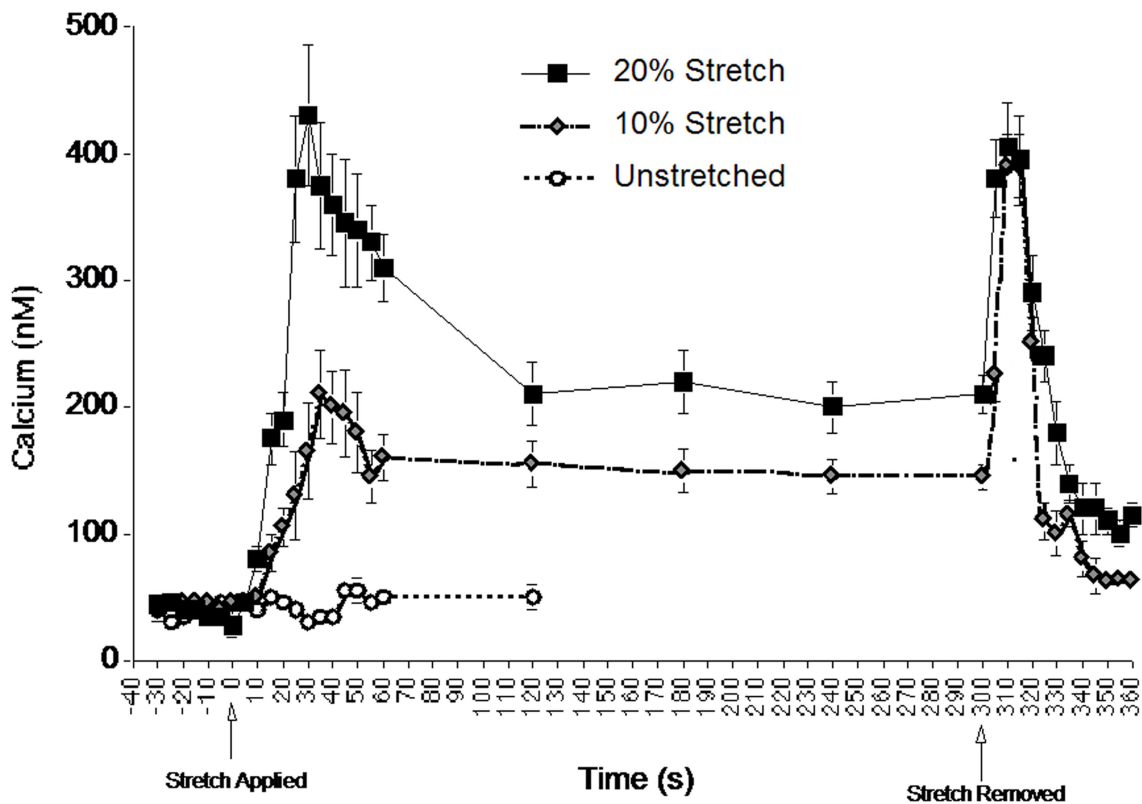


Figure 2A

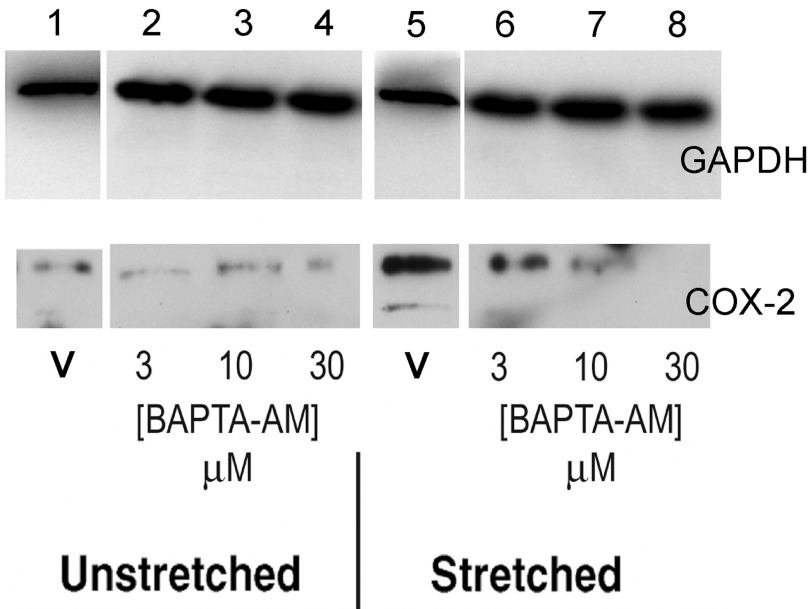


Figure 2B

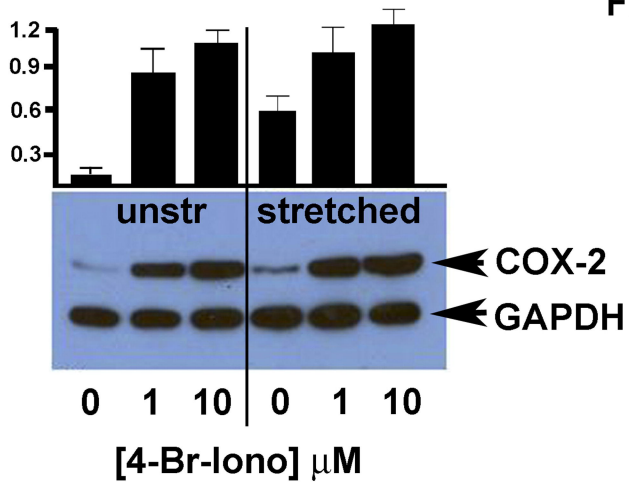
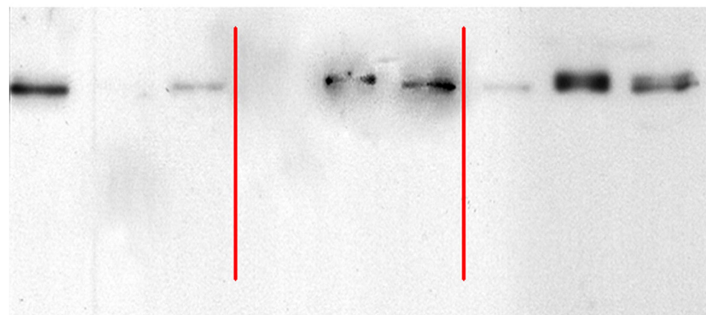
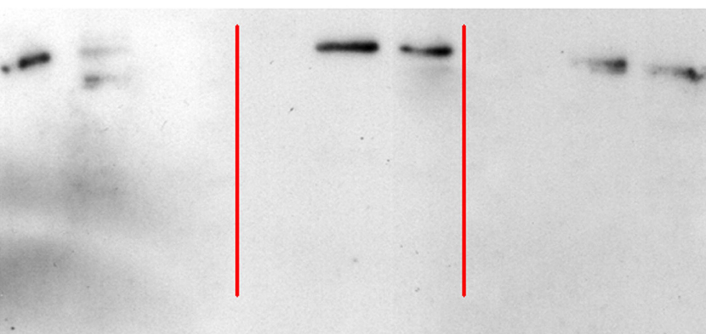


Figure 3A

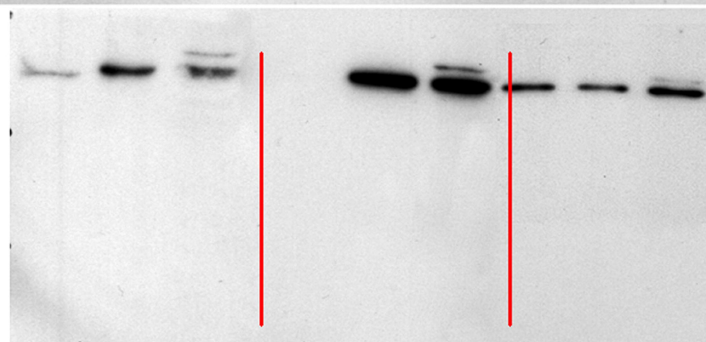
**Control    Stretch    PMA**  
**C M N    C M N    C M N**



**PKC $\alpha$**



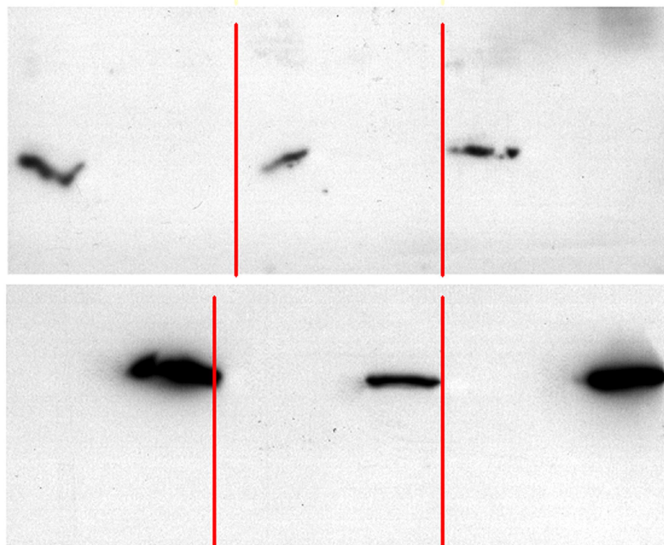
**PKC $\beta$ 1**



**PKC $\zeta$**



**Control    Stretch    PMA**  
**C M N    C M N    C M N**



**Lac DH**

**Nuc  
Lam B1**

**Figure 3B**

Figure 3C

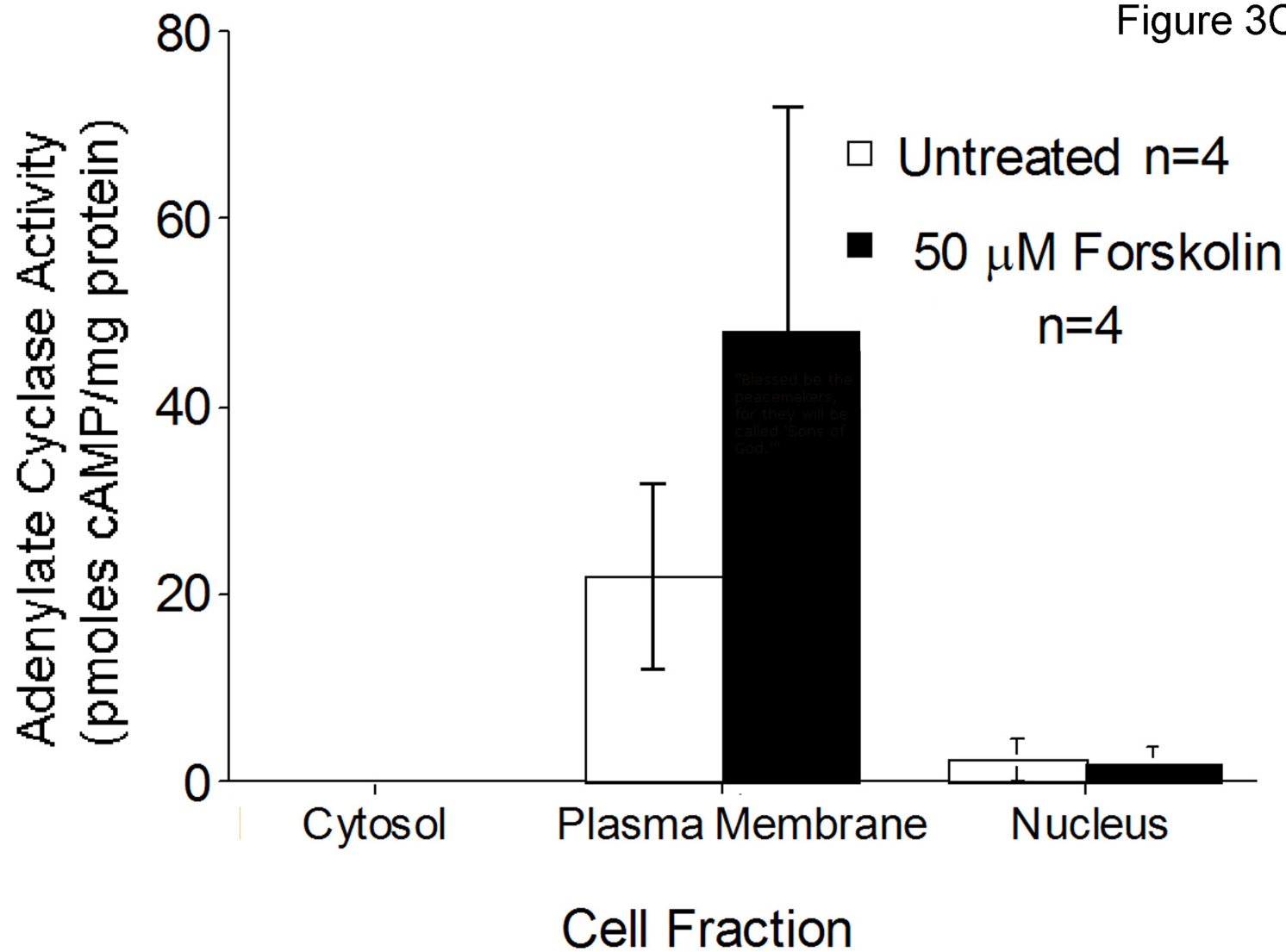


Figure 4A

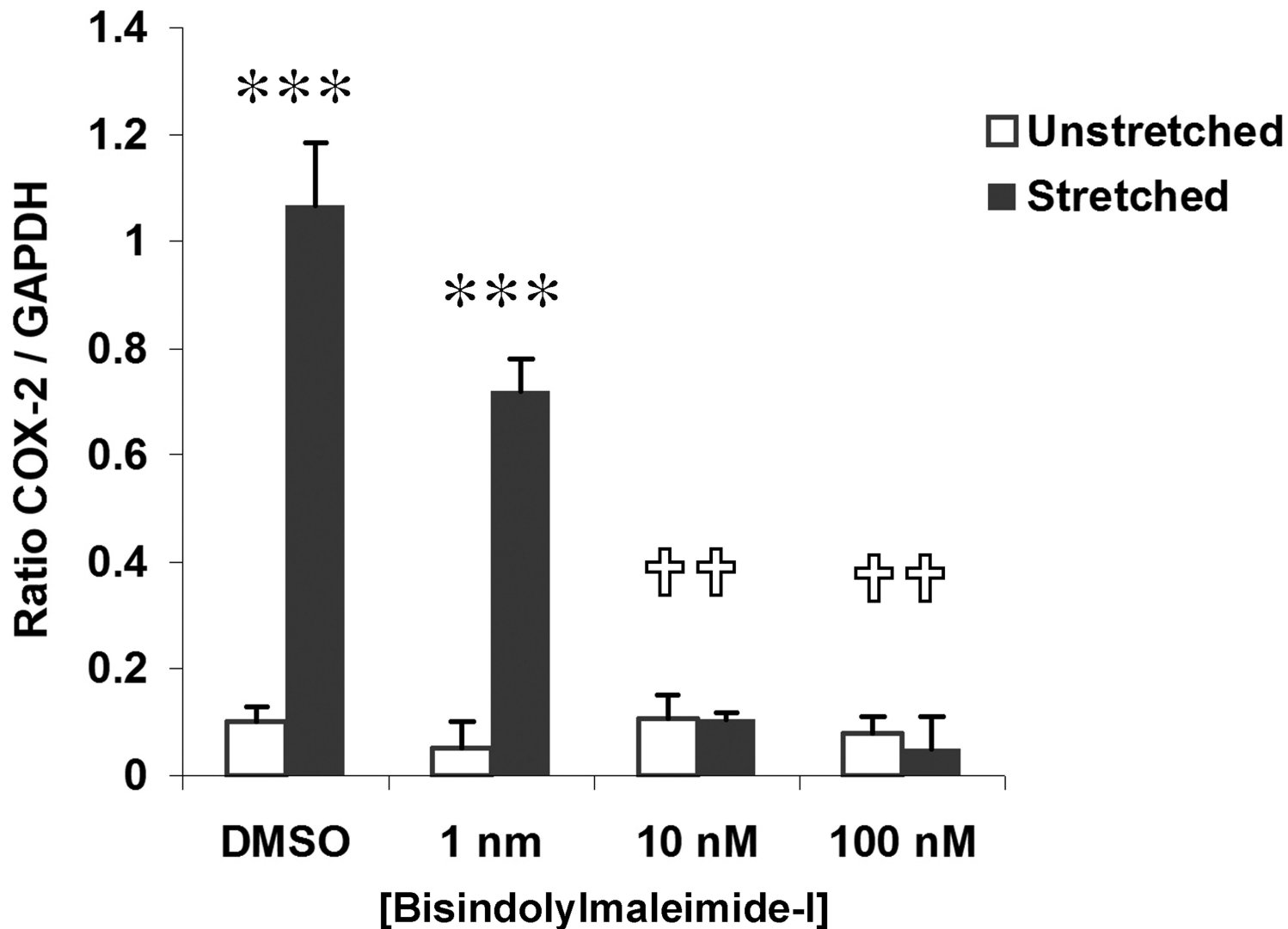
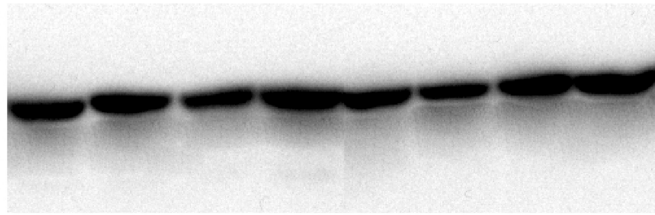
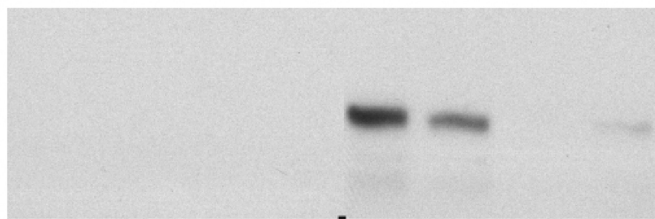


Figure 4B



GAPDH



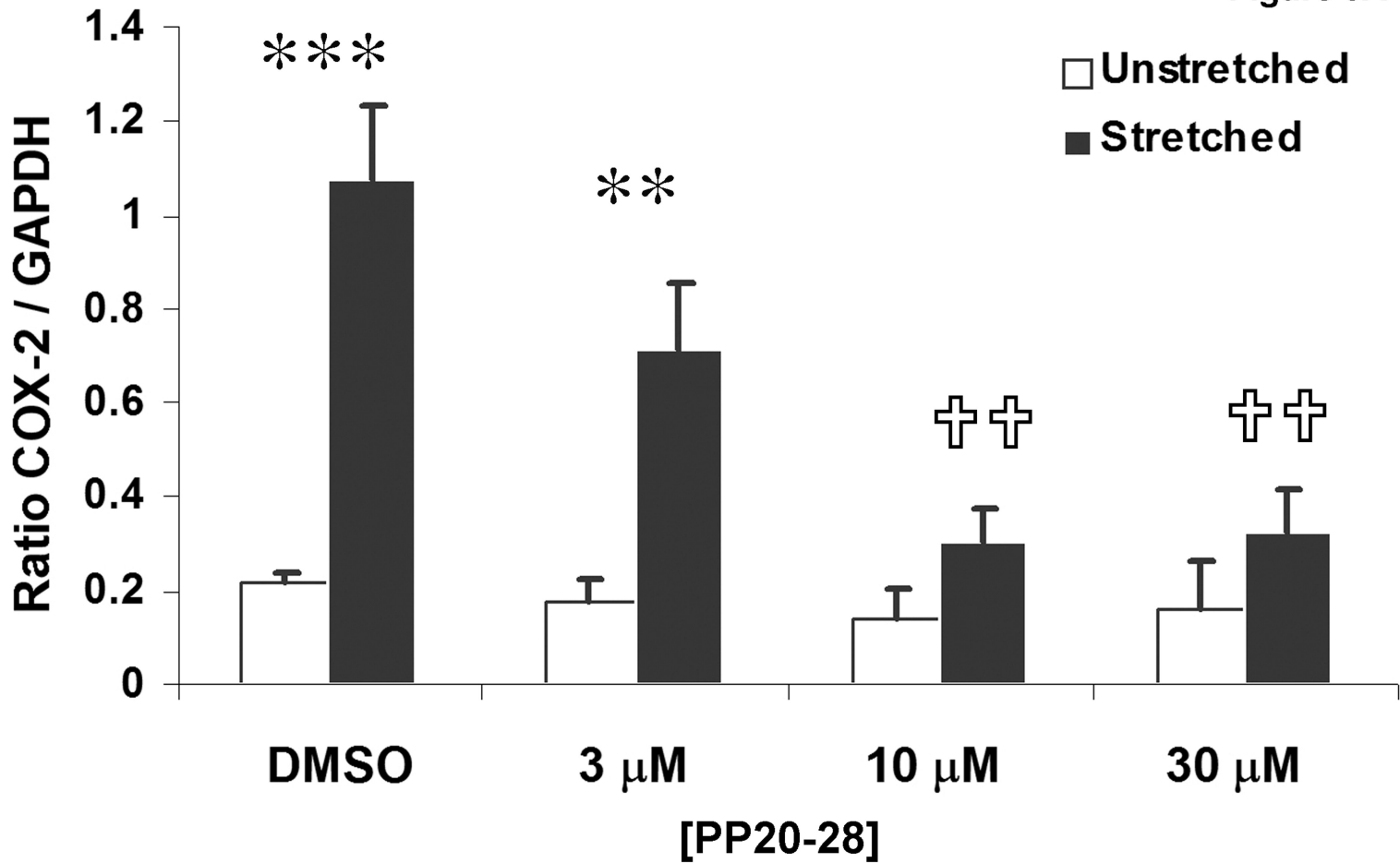
COX-2

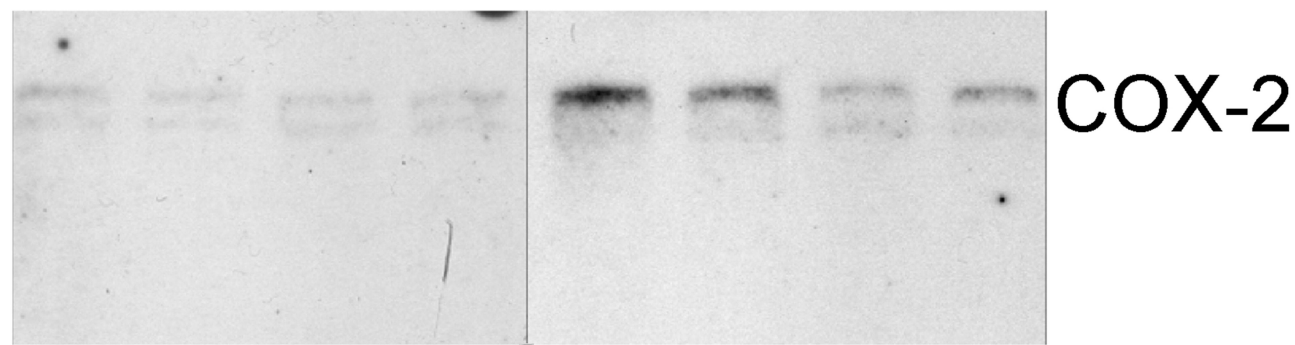
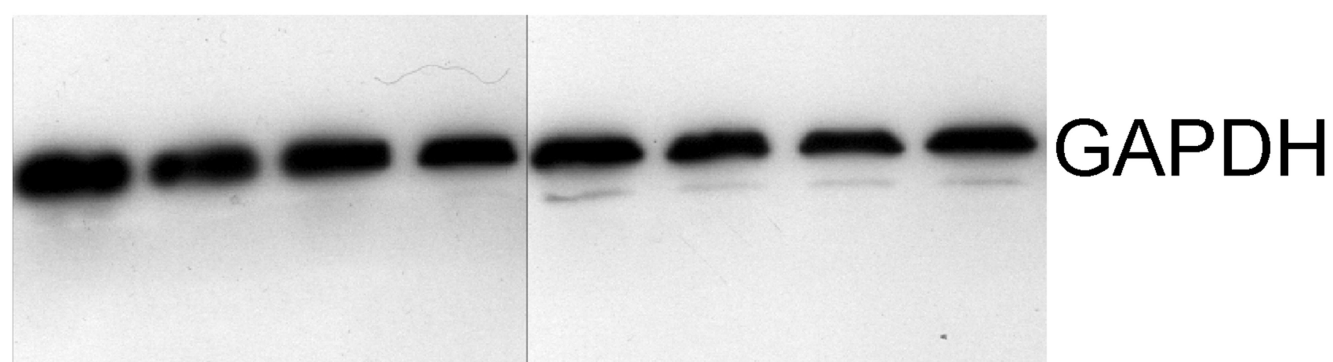
|   |            |
|---|------------|
| D | 1, 10, 100 |
| M |            |
| S | BIS        |
| O |            |

Unstretched

|   |            |
|---|------------|
| D | 1, 10, 100 |
| M |            |
| S | BIS        |
| O |            |

Stretched





D 3 10 30  
M [PP20-28]  $\mu\text{M}$   
S  
O

D 3 10 30  
M [PP20-28]  $\mu\text{M}$   
S  
O

Unstretched

Stretched

Figure 5B

Figure 6A

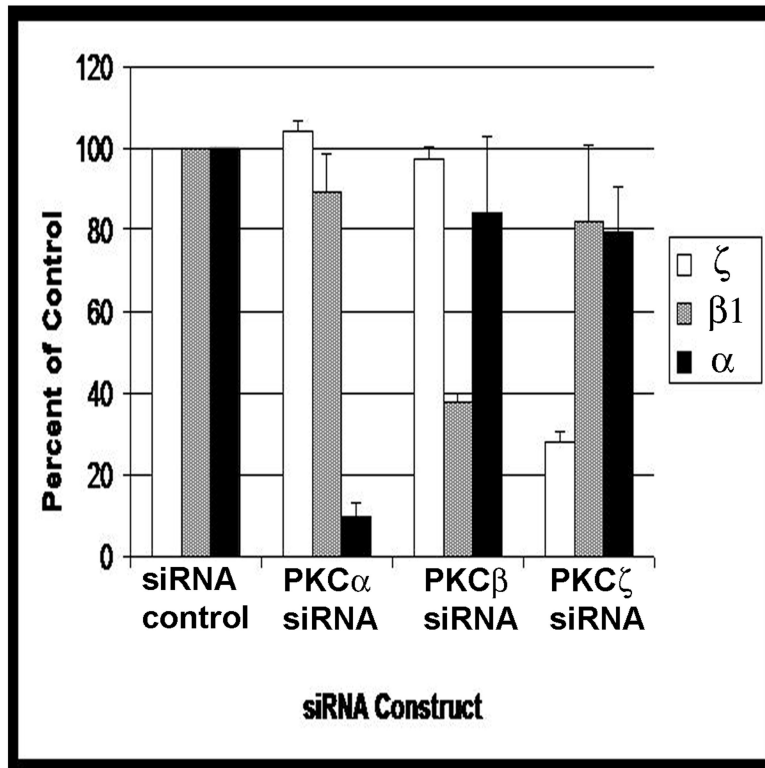
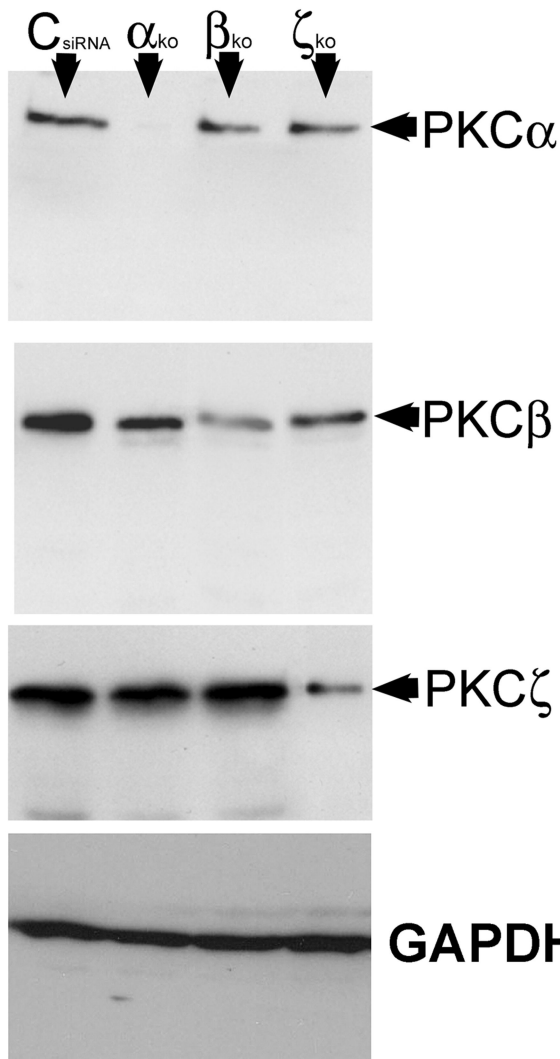
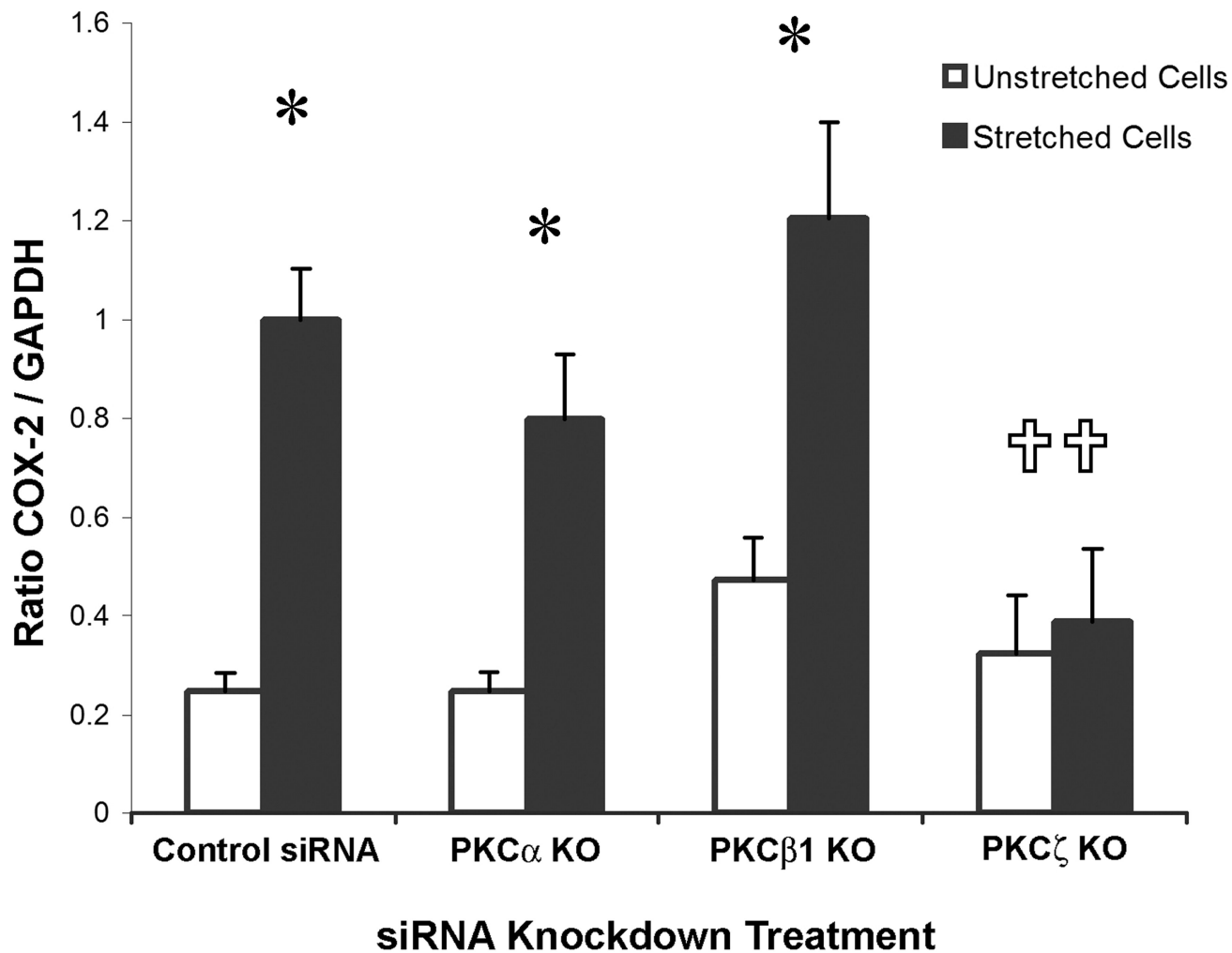


Figure 6B





Unstretched

Stretched

$\alpha$   
K  
 $\beta$   
K  
 $\zeta$   
K

$\alpha$   
K  
 $\beta$   
K  
 $\zeta$   
K

C O O O

C O O O

GAPDH

COX-2

Figure 6C

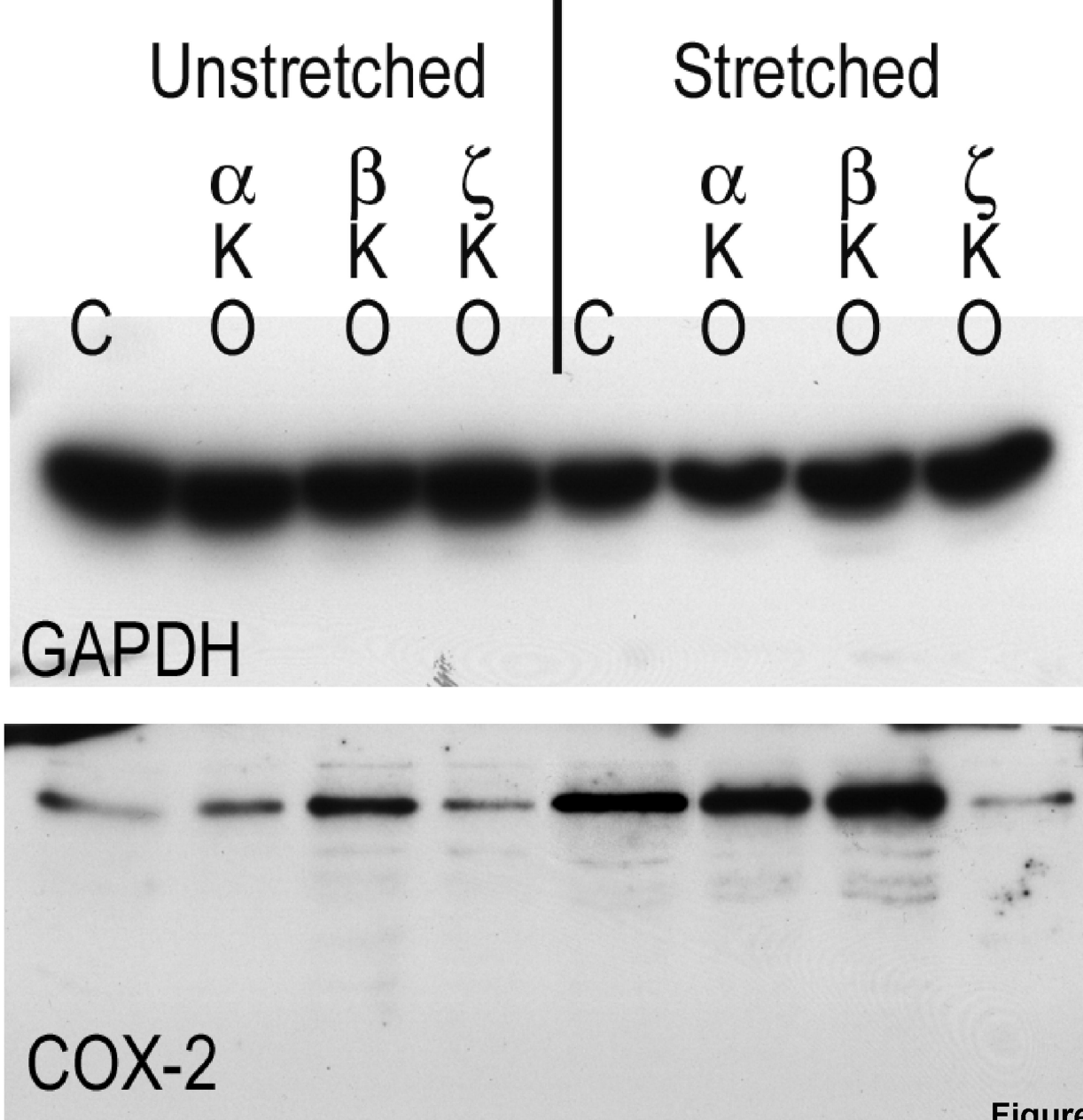


Figure 7.

